Journal of Geodynamics 59–60 (2012) 207–218

Contents lists available at SciVerse ScienceDirect

Journal of Geodynamics

journal homepage: http://www.elsevier.com/locate/jog

The seismically active Andean and Central American margins: Can satellite gravity map lithospheric structures?

N. Köther[a,*], H.-J. Götze[a], B.D. Gutknecht[a], T. Jahr[b], G. Jentzsch[b], O.H. Lücke[a], R. Mahatsente[a], R. Sharma[b], S. Zeumann[b]

[a] Institute of Geosciences, Department of Geophysics, CAU Kiel, 24118 Kiel, Germany
[b] Institute of Geosciences, Applied Geophysics, FSU Jena, 07737 Jena, Germany

ARTICLE INFO

Article history:
Received 30 September 2010
Received in revised form 2 November 2011
Accepted 8 November 2011
Available online 17 November 2011

Keywords:
Satellite gravity and gradient data resolution
Density and dynamic modelling
Asperity mapping

ABSTRACT

The spatial resolution and quality of geopotential models (EGM2008, EIGEN-5C, ITG-GRACE03s, and GOCO-01s) have been assessed as applied to lithospheric structure of the Andean and Central American subduction zones. For the validation, we compared the geopotential models with existing terrestrial gravity data and density models as constrained by seismic and geological data. The quality and resolution of the downward continued geopotential models in the Andes and Central America decrease with increasing topography and depend on the availability of terrestrial gravity data. High resolution of downward continued gravity data has been obtained over the Southern Andes where elevations are lower than 3000 m and sufficient terrestrial gravity data are available. The resolution decreases with an increase in elevation over the north Chilean Andes and Central America. The low resolution in Central America is mainly attributed to limited surface gravity data coverage of the region.

To determine the minimum spatial dimension of a causative body that could be resolved using gravity gradient data, a synthetic gravity gradient response of a spherical anomalous mass has been computed at GOCE orbit height (254.9 km). It is shown that the minimum diameter of such a structure with density contrast of 240 kg m^{-3} should be at least ~45 km to generate signal detectable at orbit height. The batholithic structure in Northern Chile, which is assumed to be associated with plate coupling and asperity generation, is about 60–120 km wide and could be traceable in GOCE data. Short wavelength anomalous structures are more pronounced in the components of the gravity gradient tensor and invariants than in the gravity field.

As the ultimate objective of this study is to understand the state of stress along plate interface, the geometry of the density model, as constrained by combined gravity models and seismic data, has been used to develop dynamic model of the Andean margin. The results show that the stress regime in the fore-arc (high and low) tends to follow the trend of the earthquake distributions.

1. Introduction

Novel satellite gravity missions aim at a breakthrough in recovering signals associated with mass transport, mass distribution and the underlying dynamic processes on the Earth's surface, the lithosphere and upper mantle. The missions significantly improved the coverage and availability of gravity data. In the year 2000, CHAMP started to measure the global gravity field with a spatial resolution of about 550 km (e.g. Eigen-2, Reigber et al., 2005). The following GRACE mission measured gravity with an increased spatial resolution of approximately 140 km (ITG-GRACE03s, Mayer-Guerr, 2007). In 2009, the GOCE mission has begun measuring the gradients of the gravity field. Compared to scalar measurements, gradiometry offers better signal to noise ratio, de-emphasises regional trends (Holstein et al., 2007) and provides enhanced sensitivity of geological structures (e.g. Pedersen and Rasmussen, 1990; Fedi et al., 2005). Thus, the direct use of gradients is a new scope for geophysical modelling. However, it has to be determined whether the resolution of downward continued GOCE gradient data is sufficient for direct application to lithospheric studies. One recent high-resolution gravity model of GOCE is GOCO-01s which is a combined model of GRACE solutions for lower degrees and GOCE data for higher degrees (Pail et al., 2010). Higher resolution is provided by combined models of terrestrial and satellite data. The EIGEN-5C (Förste et al., 2008) and the EGM2008 (Pavlis et al., 2008) provide gravity data with spatial resolution of 56 km and 10 km, respectively.

In this paper, we investigate the resolution and quality of various geopotential models as applied to lithospheric structures and

* Corresponding author. Tel.: +49 431 880 1517; fax: +49 431 880 4432.
E-mail address: nkoether@geophysik.uni-kiel.de (N. Köther).

0264-3707/$ – see front matter © 2011 Elsevier Ltd. All rights reserved.
doi:10.1016/j.jog.2011.11.004

mapping of regions of high seismic moment release (asperities) using the active plate boundaries of Central America and Southern Central Chile as case studies. The origin and role of asperities in earthquake recurrence in these regions are much debated (e.g. Wells et al., 2003). Many source time functions of large earthquakes show distinct onsets of sub-events and episodes of moment release, which signify co-seismic failure of asperities. As causes for these sub-events, varying physical properties such as geometrical and/or material heterogeneities and dynamically generated complexities are suggested (Madariaga and Cochard, 1996; Aochi et al., 2003; Marsan, 2006). Inhomogeneities on the subducting plate (e.g. seamounts, ridges, transform faults) could lead to stronger coupling (Cloos, 1992; Kirby et al., 1996; Barckhausen et al., 1998; DeShon et al., 2003). Deep-sea terraces and sedimentary basins along convergent margins are other proposed indicators of asperities (Song and Simons, 2003; Wells et al., 2003; Fuller et al., 2006).

In regions of high seismic moment release, trench-parallel gravity anomalies positively correlate with topography. Thus, the spatial gravity variations over the fore-arc could serve as proxy for the long-term state of stress on the plate interface (Song and Simons, 2003). Furthermore, Wells et al. (2003) showed that epicentres of major earthquakes often tend to concentrate on the pronounced gravity gradients from the fore-arc basins towards gravity highs. Recent studies in the South-Central Chile suggest that pressure exerted by batholitic structure and buoyancy force acting on the Nazca plate could be one of the possible mechanisms of asperity generation (Sobiesiak et al., 2007). An analysis of the 1995 Antofagasta earthquake showed that high b-values correlate with isostatic residual gravity anomalies of the region (Sobiesiak et al., 2007). The isostatic residual anomalies are caused by batholitic bodies of the Jurassic to early Cretaceous magmatic arc system and help to lock the interface of the seismogenic zone. This is also indicated in the local tomography as high P-wave velocity (Husen, 1999). Tassara (2010) expanded this hypothesis for the entire Chilean-Pacific margin and suggested that hazardous earthquakes predominantly occur in regions of positive vertical stress anomalies associated with positive density anomalies of the crust in the fore-arc region.

The scope of this work is to test the resolution of satellite-only and combined models as applied to lithospheric structure, tectonic processes and dynamic evolution of convergent plate boundaries. In order to test the resolution and unravel the 3D structure as well as the dynamic evolution of the two convergent plate margins, three steps have been followed: (1) all terrestrial gravity data from the region of interest have been combined into a single database; (2) satellite-derived gravity data have been used to fill in regions lacking terrestrial gravity coverage; and (3) the combined gravity database has been used to develop 3D lithospheric structures of the two convergent plate margins. Then, the geometry and physical parameters obtained from the well-constrained 3D density models have been used to refine the dynamic models of the Andean margin. The satellite gravity data have been obtained from the ICGEM portal of the GFZ Potsdam (http://icgem.gfz-potsdam.de/ICGEM/).

2. Tectonic setting

The Andes mountain belt is the result of subduction of the Nazca beneath South America plate. The dynamics of subduction are mainly controlled by the convergence rate and age of the subducting plate. Several studies indicate the differences in tectonic style between the Central and Southern Andes (e.g. Allmendinger et al., 1997; Ramos and Aleman, 2000). The Central Andes can be divided from west to east into the fore-arc, magmatic arc and backarc (Reutter and Götze, 1994). The fore-arc comprises the Coastal Cordillera, the Longitudinal Valley, the Precordillera and the Preandean depression (Fig. 1). Since the Jurassic, the magmatic arc front has migrated more than 200 km to the east (e.g. Scheuber et al., 1994), with the Jurassic arc now present along the Coastal Cordillera and on the slope of the fore-arc (about 50–150 km east of the trench). Repeated micro-gravity and GPS measurements reveal the on-going deformation and relaxation processes after the 1960 Valdivia earthquake (Klotz et al., 2001). The main causes for these tectonic differences are changes in slab dip, age and convergence obliquity (e.g. Gutscher et al., 2000). Young and buoyant slabs produce shallow dips and strong seismic coupling. Convergence was always oblique, with obliquity changing with time and latitude. Convergence velocity also fluctuated considerably and has been decreasing throughout the Neogene (Norabuena et al., 1999). However, it was always amongst the faster convergence rates observed on Earth.

In this paper, we will focus on the structures and processes affecting the fore-arc region. For comparison, we will use the gravity field and results of the density modelling from Central America. Therefore, we provide a brief introduction to the geology of the region. For more detail, refer to Lücke et al. (2010). The outstanding tectonic feature is the subduction of the oceanic Cocos plate beneath the Caribbean plate along the Middle American Trench. Throughout Central America, the volcanic front is segmented along the isthmus presenting gaps in Quaternary volcanism as well as changes in distance from the Middle American Trench. Such changes have been attributed to both the state of stress in the overriding plate and the disposition of the subduction zone leading to changes in depth to the slab (Bolge et al., 2009). The heterogeneity of the structure of the oceanic Cocos plate due to the influence of the Galapagos hot-spot (Sallarès et al., 2003) leads to inconsistencies upon the arrival of bathymetric features to the subduction zone and may cause seismogenic asperities and uplift (Barckhausen et al., 1998; Meschede et al., 1998). Furthermore, the subduction of seamounts on the oceanic Cocos plate acts as an agent of upper plate erosion (Ranero and von Huene, 2000). At the western end of the Middle American Trench, the plate boundary between the Cocos and Nazca plates is marked by the seismically active Panama Fracture Zone. Subduction of the Nazca plate along the southern Panama segment is now considered to be inactive showing instead evidence of left lateral shearing between the Nazca and Caribbean plates (Lonsdale, 2005).

3. Gravity database and geophysical constraints

Onshore gravity data collected under the framework of the Collaborative Research Centre 267 (Oncken et al., 2006) have been homogenized to compile Bouguer anomaly map of the Central Andes. The database comprises data acquired over the past 30 years in Argentina, Chile and Bolivia (20°S–29°S and 74°W–64°W). Approximately 2000 gravity stations covering the region in Argentina between the Andes and the Atlantic coast were measured along the southern traverse in 2000 (36°S–42°S and 71°W–62°W) and along the northern traverse between 1982 and 1990 (Götze et al., 1994; Schmidt and Götze, 2006; Hackney et al., 2006; Alasonati-Tašárová, 2007). Additional data have been obtained from industry (ENAP; Chile and Repsol-YPF; Argentina), the Universidad de Chile and the United States National Imagery and Mapping Agency. All measurements are tied to the IGSN71 gravity datum. Bouguer anomalies were computed using the normal gravity formula of 1967 and a spherical Bouguer cap correction (cap radius 167 km, density 2670 kg m^{-3}). Terrain corrections on land were computed using triangular facets to approximate topography up to a distance of 167 km from stations. The corrections were applied using the 1 km × 1 km GLOBE (onshore) and ETOPO5 (offshore) digital elevation models. Offshore gravity and seismic data are obtained from shipborne measurements of the SPOC (Subduction Processes Off Chile) project (e.g. Reichert and Schreckenberger,

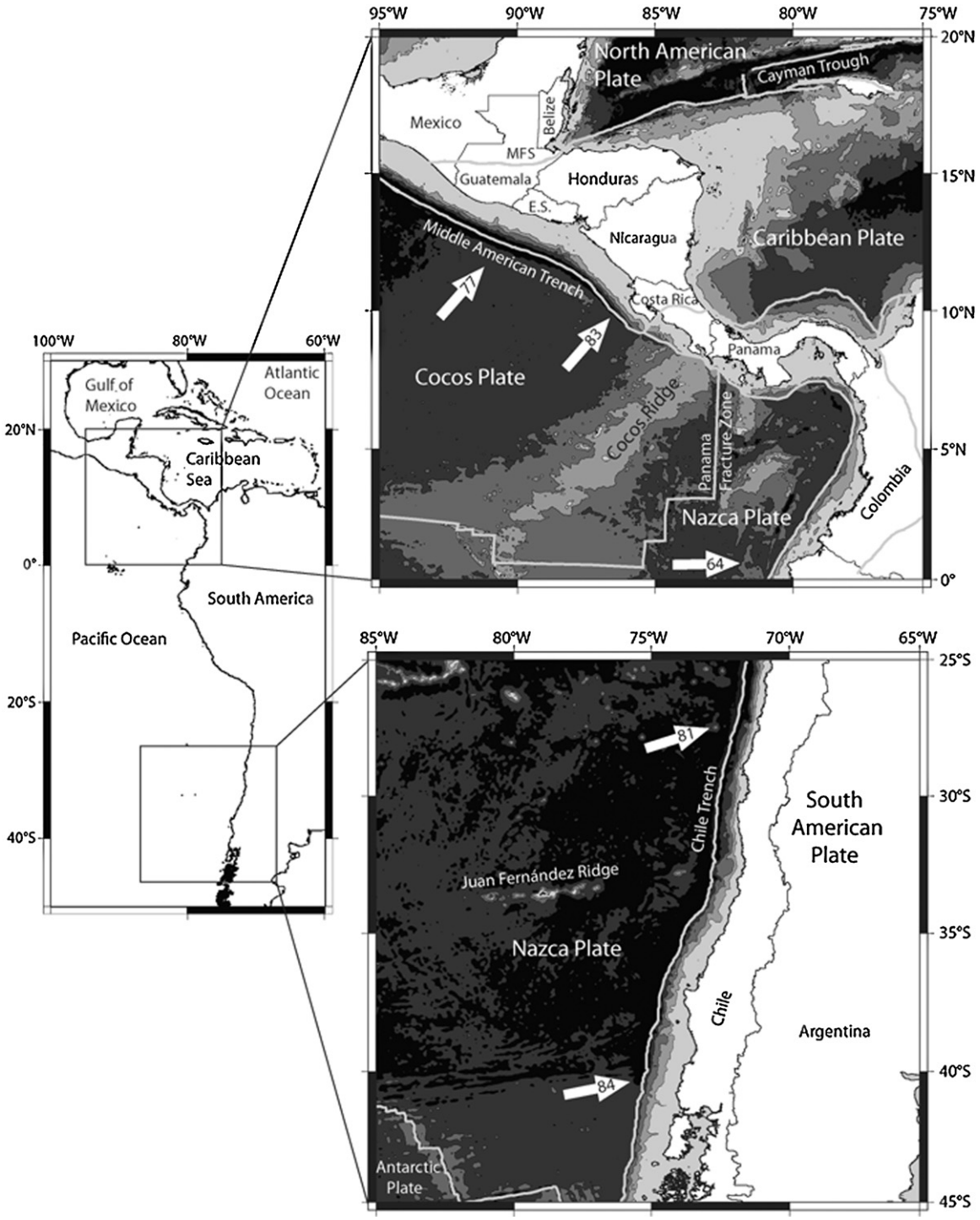

Fig. 1. Geologic setting of Central (top) and South (bottom) America. The white arrows show the plate movement per year in mm (DeMets et al., 1994). Grey lines offshore indicate plate boundaries. Dark colours indicate deep, light colours shallow seafloor.

2002). The former are merged with the KMS-2001 global free-air gravity anomaly database (Andersen and Knudsen, 1998). The Bouguer anomaly in the Central Andes has a resolution of $3–5 \times 10^{-5}$ m s^{-2}.

A series of 3-dimensional density models showing mass distributions at different scales in the western continental margin of South America have previously been developed (Kirchner et al., 1996; Tassara et al., 2006; Alasonati-Tašárová, 2007; Prezzi et al., 2009). Tassara et al. (2006) presented a sub-global density model (410 km depth) encompassing the Pacific Ocean (85°W) and the Andean margin between the northern Peru (5°S) and Patagonia (45°S). At a regional scale, 3D density models of the Central (between 36°S and 43°S) and South Central Andes have been developed by Kirchner et al. (1996), Alasonati-Tašárová (2007) and Prezzi et al. (2009). All models traverse the Andes and provide complete picture of lithospheric density distributions. Modelling was done using the 3D gravity modelling package IGMAS (Götze and Lahmeyer, 1988; Schmidt et al., 2010). Model constraints were

taken from active and passive seismic campaigns conducted under the framework of the Collaborative Research Centres 267 (Giese et al., 1999; Oncken et al., 2006; Sick, 2006) and 574 (Ranero et al., 2003; Brasse et al., 2009). Moreover, results of the previous seismic experiments from PISCO (Proyecto de Investigación Sismológica de la Cordillera Occidental; Lessel, 1997; Schmitz et al., 1999), ANCORP (Andean Continental Research Program; ANCORP Working Group, 2003; Buske et al., 2002) and ISSA (Integrated Seismological experiment in the Southern Andes; Bohm et al., 2002; Lüth et al., 2003) have been used to constrain major structures such as Moho, upper slab surface, lithosphere–asthenosphere boundary and intra-crustal inhomogeneities.

For Central America, a similar database was compiled and homogenized. Offshore databases consisting of ship borne gravity and seismic data acquired within the activities of the Collaborative Research Centre 574 have been used to cover mainly the area along the Middle American trench and the Pacific continental shelf. Seismic reflection, refraction and tomography data sets provided constraints for the modelling (Sallarès et al., 2001, 2003; Husen et al., 2003; Arroyo et al., 2009). The onshore gravity database was also compiled by SFB574 members and consists of data from various government and academic institutions. Bouguer and terrain corrections were carried out following similar processing procedures as for the Andean gravity dataset.

4. Results and discussions

4.1. Geophysical and geodetic Bouguer anomaly

The definition of Bouguer anomalies is different in Geophysics and Geodesy. In order to avoid confusion, the differences between "gravity anomalies" and "gravity disturbances" will be explained. Detailed discussions about this issue can be found in the work of Li and Götze (2001) and Hackney and Featherstone (2003). In general, for geophysical interpretation and modelling, "geophysical Bouguer anomalies" will be used. Here, the measured gravity is corrected for the normal gravity formula at station elevation as well as for the Bouguer slab and the topographic variations. The measured gravity value is still interpreted at its original height (Fig. 2). In terms of geodesy, gravity values that are corrected for the normal gravity but still defined at station elevation are called disturbances. The Bouguer anomaly provided by the ICGEM is defined as the gravity calculated at the geoid and corrected for both the normal gravity at the ellipsoid and a plain Bouguer slab (called "classic anomaly" according to ICGEM terms; Fig. 2; Barthelmes, 2009). In the discussions to follow, we will continue to call this the "geodetic Bouguer anomaly". Downward continuation of the geodetic Bouguer anomaly to the geoid is only valid when it is assumed that all singularities of the gravity field lie below the geoid. This is not the case in regions of high topography. Furthermore, density anomalies located between the geoid and the top of the topography are of interest for geophysical interpretation. Hence, differences between geophysical and geodetic Bouguer anomalies can be high. Moreover, the use of disturbances (geophysical anomalies) is consistent with reduction techniques of existing geophysical terrestrial datasets. Thus, the geophysical Bouguer anomaly should be used in regions of high topography.

4.2. Data quality of the EGM2008

The EGM2008 consists of GRACE satellite data up to a spatial resolution of approximately 140 km. Data from 140 km spatial resolution up to 10 km are derived from other sources such as terrestrial, satellite altimetry and "fill-in" data (Pavlis et al., 2008). Regarding the additional onshore data, several inconsistencies appear

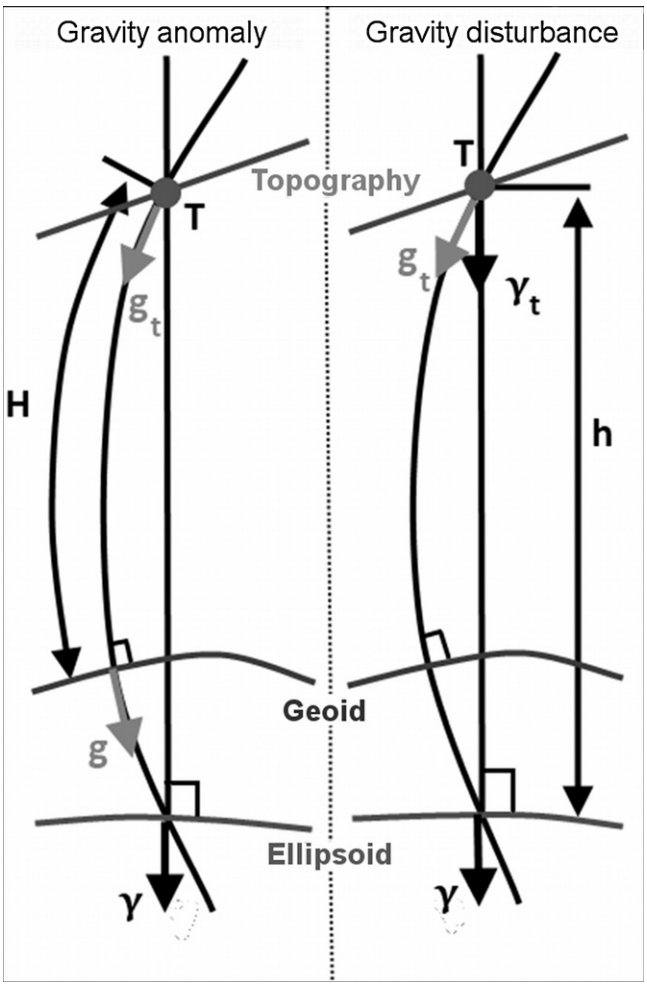

Fig. 2. Gravity anomaly and gravity disturbance. The gravity anomaly (left) is downward continued from the observation point T to the geoid (g_t to g) and then reduced by the normal gravity from the ellipsoid (γ). Downward continuation is an unstable procedure over mountainous regions. Gravity disturbance (right) can be determined at any level (g_t) and is reduced by the upward continued normal gravity value (γ_t). This procedure is stable.

because its availability and distribution is not homogeneous. Moreover, in areas void of any terrestrial gravity data, "fill-in" data were used. These datasets were synthesized from GRACE data and augmented with data from the EGM96 and gravity derived from topography by means of residual terrain model (RTM) (Pavlis et al., 2007). At locations, where confidential terrestrial gravity datasets are available, the data were used up to the maximum resolution permitted by the restrictions and then augmented with RTM anomalies. This approximated gravity solution lacks high frequency anomalies (>degree 1650; Pavlis et al., 2007). For the present study, we used terrestrial datasets collected by Schmidt and Götze (2006). It is expected that these data are included in the EGM2008. Thus, the EGM2008 should correlate well with the surface data at its maximum spatial resolution. If the data do not coincide, errors or inconsistencies in the EGM2008 may be assumed.

In the Andes, two onshore areas with different topography were investigated: The North Chilean part is located between 74°W–67°W/19°S–30°S. Elevation in this region reaches up to 5800 m above sea level. The southern part (between 73°W–60°W and 36°S–43°S) has elevations up to 3000 m. In Central America, the study area is located between 86.5°W–82°W/8°N–11.5°N with elevations up to 3800 m. The number of onshore gravity stations

Table 1
Correlation of the EGM2008 with terrestrial data. The maximum deviations of each model are shown. The correlation values in brackets are for the Andes west of 69°W. Thus, only stations located around mountainous areas and the coastal line are considered. In Costa Rica, the brackets show the correlation of stations located above 1000 m of altitude.

	North Andes (19°S–30°S) onshore		South Andes (36°S–43°S) onshore		Central America onshore	
	Geophysical BA	Geodetic BA	Geophysical BA	Geodetic BA	Geophysical BA	Geodetic BA
Correlation between EGM2008 and terrestrial data (%)	99.48 (98.29)	98.91 (95.63)	96.51 (93.26)	97.48 (94.32)	85.8 (49.37)	68.2 (40.66)
Min. Deviation ($\times 10^{-5}$ m s^{-2})	−50	−128	−66	−77	−55	−203
Max. deviation ($\times 10^{-5}$ m s^{-2})	80	87	58	48	112	169

used for the Northern Chile, Southern Chile and Central America are 8373, 14210 and 13387, respectively.

Table 1 shows the correlation between the EGM2008 anomalies (geodetic and geophysical) and terrestrial gravity data for the Andes and Central America. In general, the EGM2008 shows high correlation (>95%) in the Andes. However, low correlation has been obtained over the regions with rough topography, where deviations of about 40% are observed (e.g. 128×10^{-5} m s^{-2}). The data correlation in Central America is even lower (about 68% deviations for the geodetic anomaly and ∼86% for the geophysical anomaly). This is mainly attributed to sparse terrestrial gravity data coverage.

Fig. 3 shows the gravity maps of Central America and the Southern Andes in which the geodetic and geophysical Bouguer anomalies are compared with terrestrial data. The histograms in Fig. 4 show the deviation of the geodetic (dotted) and geophysical (hatched) anomaly compared to the terrestrial data in the Andes. The deviation of the geodetic anomaly compared to the geophysical anomaly is larger (∼0.6%) in the northern part where topography is higher. In the southern part, the geodetic anomaly is slightly better (∼1%) than the geophysical anomaly. However, both datasets show significant deviations from the terrestrial data with values higher than 20×10^{-5} m s^{-2}.

For Central America, a three dimensional density model is being developed within the framework of the SPP1257. The density model is based on gravity data from the EGM2008 geopotential model. The results have shown that the resolution of this model is appropriate for the modelling of regional lithospheric mass distribution and major tectonic structures such as the Middle American subduction zone, the continental and oceanic Moho as well as first order crustal discontinuities represented by the heterogeneities in the crustal basement and the upper crust (see Fig. 5).

Fig. 5 shows a cross-section of the 3D density model through central Costa Rica in which different datasets are compared and put into the context of the modelled structures. In the offshore areas, a good correlation has been obtained between the EGM2008 satellite gravity model and surface data. The geophysical Bouguer anomaly (offshore) is located on the geoid (on the ocean surface). Thus, it coincides with the geodetic Bouguer anomaly. Onshore, the geophysical Bouguer anomaly shows better correlation to the surface data than the geodetic Bouguer anomaly. In the mountainous areas of Costa Rica, the geodetic Bouguer anomaly (dashed line) differs significantly from the surface data (dotted line) as well as from the geophysical Bouguer anomaly (black).

The analysis of the present study shows that rugged topography downgrades the spatial resolution of the EGM2008 featuring large outliers in the Andes and Central America. Results in Central America show that high and unexpected deviations can be present in areas void of any terrestrial gravity data. Thus, the quoted spatial resolution of 10 km is not valid for all regions. Our case studies in these regions show that in areas of rugged topography, the geophysical anomaly often provides better results (up to 9% in mountainous regions; Table 1). Moreover, the use of geophysical anomalies in the calculation is consistent with the existing reduction techniques of terrestrial geophysical datasets.

4.3. Spatial resolution of different satellite gravity models

The main geophysical objective of using satellite-derived gravity data is the interpretation of lithospheric structures. We have used a well-constrained 3D density model of the South-Central Chile (Alasonati-Tašárová, 2007) to assess the spatial resolution of different satellite gravity models. The comparison emphasizes the areas of the models in which problems may occur when using different satellite gravity models (EGM2008, EIGEN-5C, ITG-GRACE03s, and GOCO-01s).

Fig. 6 shows a section of the 3D density model from the Central Chile at 37.4°S. Also shown on the top panel are gravity fields derived from different satellite models, measured surface gravity data, and the calculated gravity field from the density model. The dashed black line illustrates the calculated gravity from the density model and the red line shows the measured surface data. The EGM2008 (black) and the EIGEN-5C (yellow) show overall good correlation with the calculated gravity field. In the area of high topography (e.g. at 100 km of the *x*-axis), the EGM2008 exhibits significant deviations. The EIGEN-5C is smoother and correlates better with the predicted field. However, a deviation of about 15×10^{-5} m s^{-2} is observed between 350 and 400 km. The same misfit is visible in the GRACE solution (dark blue). The GRACE-GOCE satellite model (light blue) provides a better fit to the calculated gravity. Here again, deviations at 200 and 420 km are observed. However, the gravity low below the Andes at 300 km is better resolved by the GRACE-GOCE model. The gravity low of the deep-sea trench is well fitted by the combined models but the GRACE model does not comprise a distinct gravity low. Compared to other models, the deep-sea trench and the root of the Andes are more visible in the GRACE-GOCE model. The Coastal Cordillera is also shown as gravity high, but not well fitted in amplitude. The new GRACE-GOCE satellite model shows the best fit. The EIGEN-5C provides a good fit over the entire section. The deviation of the EGM2008 in regions of high topography is clearly visible in areas where no surface data is available. The higher degree models such as the EGM2008 and EIGEN-5C cannot provide a high spatial resolution.

Overall, the GRACE-GOCE model shows an increased spatial resolution relative to the GRACE derived field. Since large-scale density models do not resolve local features, the calculated gravity field is smooth and comparable with wavelengths obtained from satellite-only gravity models. Combined models with new GOCE data could be sufficient for compiling density models of regional scale in frontier regions. Although combined gravity models can be used for density modelling of relatively smaller features such as shallower crustal structures, satellite-only models are not appropriate for this purpose due to the low spatial resolution.

4.4. Asperity mapping and resolution of gravity gradient data

Delineation of potentially hazardous provinces using gradiometry is one of our objectives. In order to examine the applicability of GOCE gradients for asperity detection in a simple way, the minimum dimension of a spherical anomalous mass below the geoid

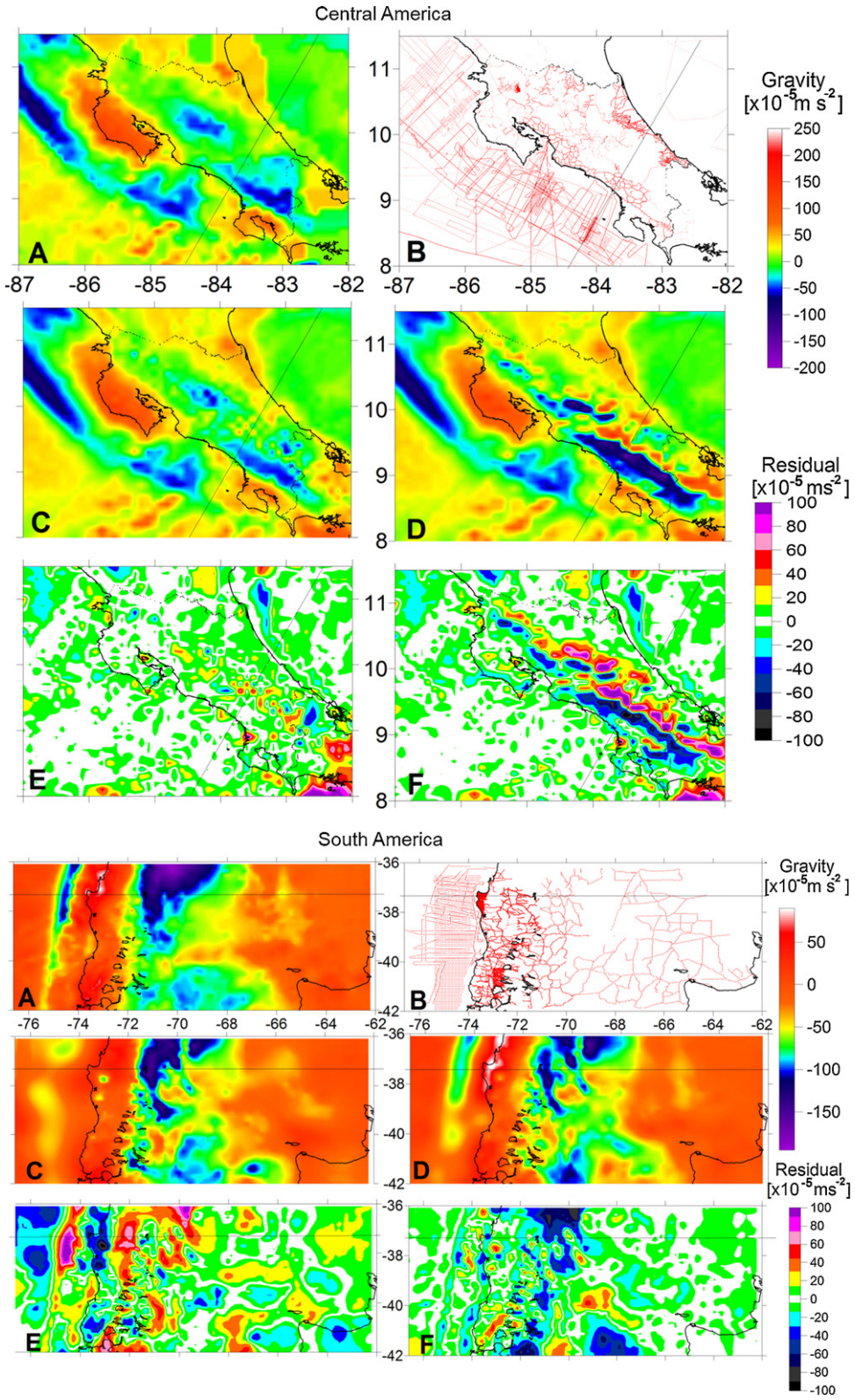

Fig. 3. Comparison of the EGM2008 with surface gravity data from Costa Rica (top) and Chile (bottom). (a) Data from surface stations with Bouguer gravity anomaly on-shore and free-air gravity anomaly off-shore; (b) location of surface stations; (c) geophysical Bouguer anomaly (from EGM2008); (d) geodetic Bouguer anomaly (from EGM2008); (e) residual map obtained by subtracting (a) from (c); (f) residual map obtained by subtracting (a) from (d). Bold black lines show the coastline and borders. Straight line shows location of cross-section of the 3D density model shown in Figs. 5 and 6.

producing gravity and gravity gradient amplitudes of the order of GOCE's accuracy at orbit height (254.9 km) has been calculated. The curves in Fig. 7 show the minimum diameter of such a mass of given density contrast required to produce signal differences of 1×10^{-5} m s^{-2} and 12×10^{-12} s^{-2} at orbit height. These values are close to the expected accuracies of the gravity and vertical gravity gradient of GOCE global data, respectively (Pail, 2011, pers. comm.). As shown in Fig. 7, an anomalous structure with density contrast of

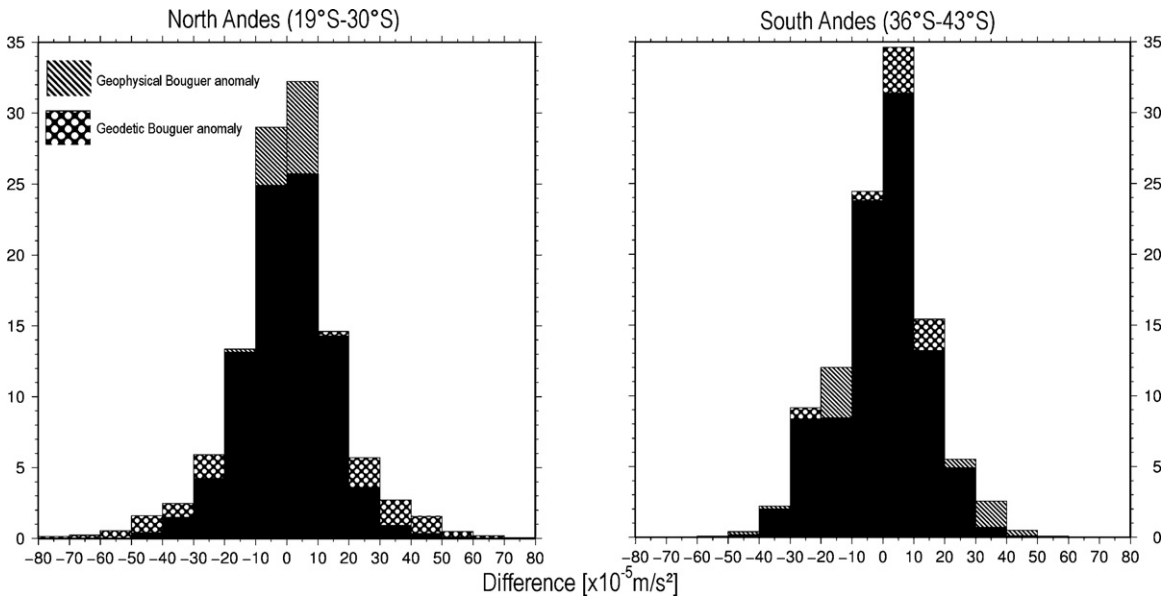

Fig. 4. The deviation of the geodetic Bouguer anomaly (dotted) and geophysical Bouguer anomaly (hatched) from terrestrial data. The area, marked in black, indicate the overlapping of both datasets. In the northern Andes, the fit of the geophysical Bouguer anomaly is better. Most values are in the range of $\pm 10 \times 10^{-5}$ m/s^2. In the southern part, the geodetic Bouguer anomaly fits much better to the terrestrial data. Thus, the resolution of the geophysical anomaly is better in areas of large topography. However, large deviations from original datasets make the EGM2008 less reliable in these regions.

240 kg m^{-3} could be detected in a gravity data at orbit height, if its diameter is at least ~45 km. However, if the diameter of an anomalous structure increases by up to 100%, its density contrast should not be less than 33 kg m^{-3} to be detected. If gradients are considered, even bodies of about half of that size could produce signal in the range of GOCE's gradient data sensitivity. The dimension of Jurassic arc batholiths in Northern Chile is about 60–120 km (Götze et al., 1994; Husen, 1999; Götze and Krause, 2002; Sobiesiak et al., 2007). This supports the idea that batholithic structures, which are assumed to be related to asperity generation, can be detected using GOCE data.

Furthermore, we set up a synthetic model of an arbitrary subduction zone for 3D-density forward modelling. The geometry and density parameters have been adapted from the models

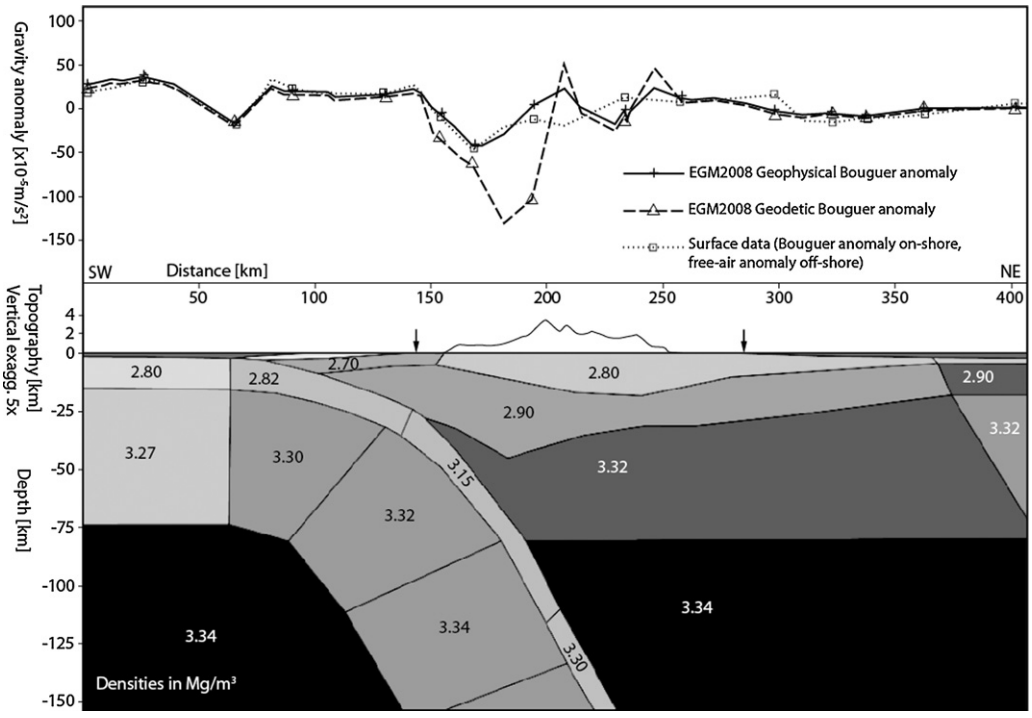

Fig. 5. Vertical cross-section of a 3D density model from Central America. Different gravity anomalies are shown in the upper panel. The dotted line (with boxes) is derived from surface gravity data and shows the geophysical Bouguer anomaly on-shore and free-air anomaly off-shore (shoreline indicated by arrows). The dashed line (with triangles) shows the geodetic Bouguer anomaly on- and off-shore calculated from the classical gravity anomaly using EGM2008 model (off-shore without Bouguer reduction). The black line (with crosses) shows the geophysical Bouguer anomaly. Offshore, all datasets correlate. Onshore, however, there is still correlation with surface data, but the geodetic Bouguer anomaly shows errors of about 80×10^{-5} m s^{-2} for this cross section. In this region, elevation reaches up to 3700 m. The errors emphasize the uncertainty of the combined gravity models and instability of the downward continuation method.

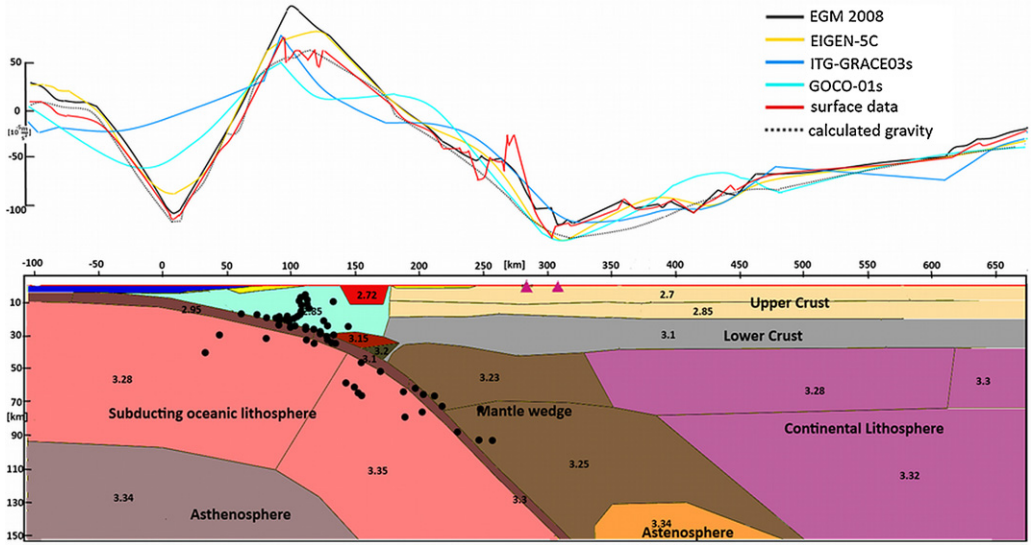

Fig. 6. Vertical cross-section of a 3D density model from Central Chile at 37.4°S (Alasonati-Tašárová, 2007). The model is constrained in part by geological and seismological information (e.g. hypocentres are shown as black circles). The dashed line shows the calculated gravity from the model matched to the surface gravity data (red curve). The combined EIGEN and EGM2008 models fit well to the data. The EIGEN-5C (yellow) correlates well with the predicted gravity values, but it also shows some deviations. The ITG-GRACE03s model does not adequately show the gravity lows of the deep sea trench (at 10 km) and crustal root (at 300 km). The GOCO-01 s (light blue) model shows the best correlation of all satellite only models.

developed by Sobiesiak et al. (2007) and Alasonati-Tašárová (2007). In order to test the signal response of asperity generating structure at different station heights using forward modelling, a three dimensional anomalous structure (115 km × 200 km × 45 km) with physical properties resembling the Chilean batholiths has been included in the modelling. A density of 3×10^3 kg m^{-3} (density contrast of 0 to 300 kg m^{-3}) has been chosen for the batholith body in the model. At the height of 254.9 km, the magnitude of the gravity gradient anomaly ranges from few to some hundred mE (1 mE = 1×10^{-12} s^{-2}). Being the second spatial derivatives of the gravity potential, gradients provide 'sharper' images of anomalies and can be combined into coordinate independent *invariants* (e.g. Pedersen and Rasmussen, 1990). Invariants sharpen density contrasts and help to emphasize structural boundaries. Fig. 8 shows how well anomalous underground structures of interest can be detected using gravity gradients at orbit height. Different tensor components give valuable information for geo-scientific interpretation. The above analysis shows that gradient maps from GOCE data may help to delineate major geological structures like fault zones, rims of sedimentary basins and intrusions.

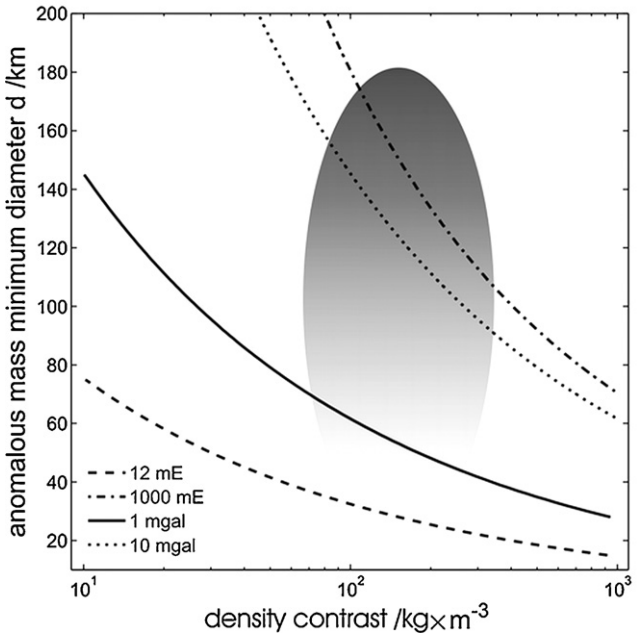

Fig. 7. Differential gravity and gradient signal caused by a minimum diameter of an anomalous spherical mass of given density contrast below geoid at an orbit height of 254.9 km. The signal is in the range of GOCE's resolution. The thick solid and dotted lines represent differential gravity signals of 1 and 10×10^{-5} m s^{-2} at an altitude of 254.9 km, respectively. The thin dashed and dash-dotted lines represent gradients of 12 and 1000 mE, respectively. The grey shaded area shows the possible combination of parameters of an asperity generating batholithic structure near subduction zones.

4.5. Geodynamic model of the Andean margin as constrained by satellite gravity data

The present mass distribution is the result of long and complex geodynamic processes. Therefore, dynamic modelling is necessary to include the effects of time factor to the static density models. The dynamic evolution of the Andean margin has been extensively studied using numerical modelling. This includes studies of the dynamics of the plateau foreland (Babeyko et al., 2006), the factors controlling the intensity of tectonic shortening (Sobolev et al., 2006) and the influence of curvature of the convergent plate margin on the stress distributions (Boutelier and Oncken, 2010). These existing models are constrained by geophysical and geological data, but are based on generalized geometries. One of the objectives of this study is to develop a dynamic model of the Andean margin using realistic geometries from a well-constrained density model. In the present study, the geometries of the 3D dynamic model have been imported from the regional 3D density model of the Andean margin (Tassara et al., 2006). The model has 16 tectonic units including the lithosphere and the upper mantle down to a depth of 410 km.

Fig. 9 shows the visco-elastic 3D dynamic model of the Andean margin. The size of the model is 1730 km × 725 km (area between 16 S–22°S and 78 W–63°W). The densities of the units have been adopted from the density model of Tassara et al. (2006). Young's moduli have been calculated using the v_p velocities from the ANCORP profile (ANCORP Working Group, 2003) and the P–S wave

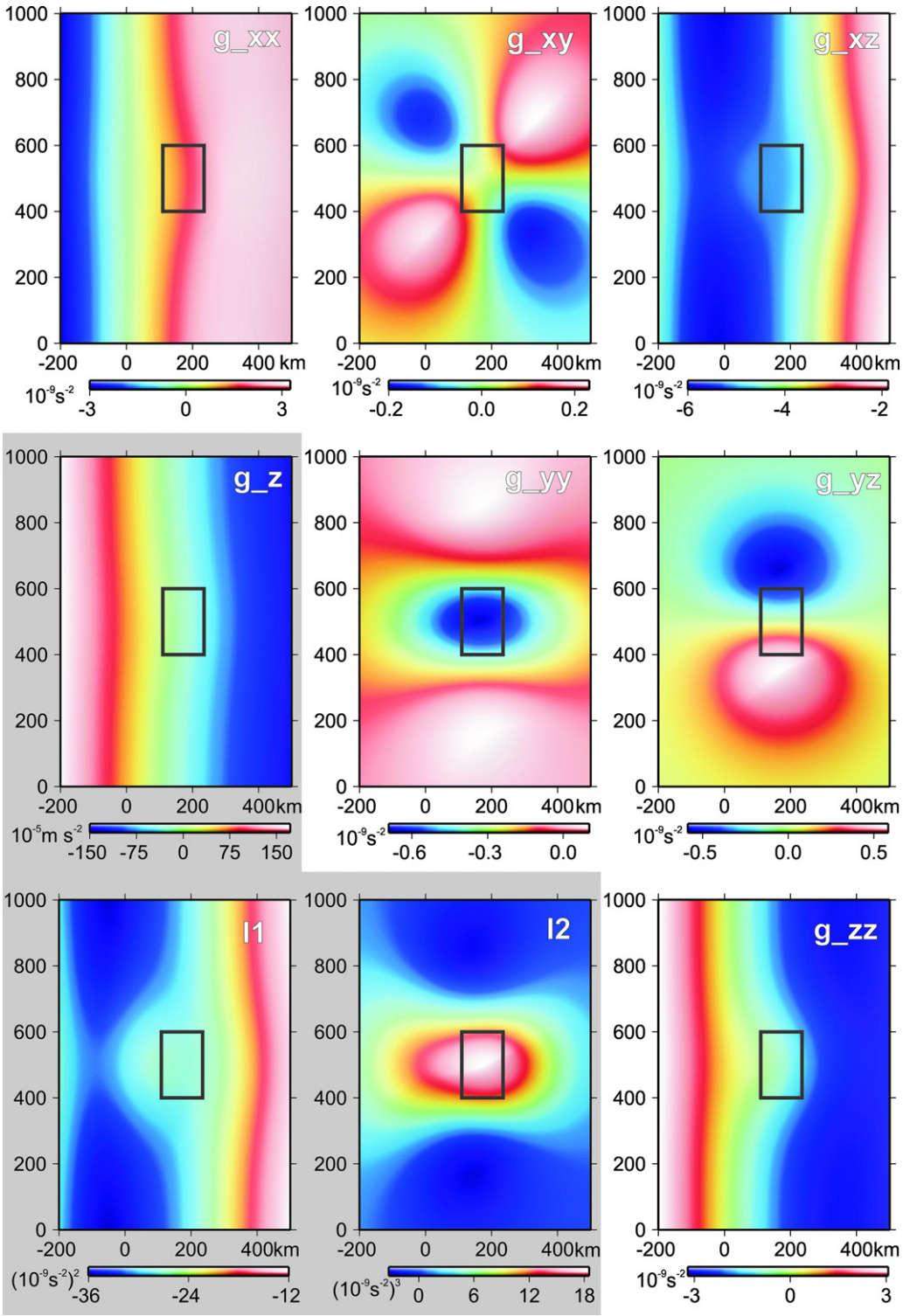

Fig. 8. 3D-Modelling of synthetic gravity (g_z), gravity gradient tensor and invariants (I1 and I2) of a subduction zone using vertical gravity field as measured at 250 km height. A batholitic structure (black box) has been included on top of the down-going slab to test the resolution of gravity gradient signal. The gradient maps emphasize the location of the batholitic structure and the general geological strike of the subduction zone.

velocity relation $v_p = 3^{1/2}v_s$. The corresponding Poisson ratio for all units is 0.25. The parameters of the geological units are shown in Fig. 9. The asthenosphere has been modelled as a viscous-elastic medium. The lithosphere is pure elastic. In the modelling, it is assumed that the South American plate is fixed and the Nazca plate moves by 7.8 cm/year for 200,000 years (Somoza, 1998). It is assumed that friction occurs only in the uppermost part of the contact up to approximately 40 km depth with a frictional coefficient of 0.1.

Beside density, however, Young's modulus, width of coupling zone, frictional coefficient and obliquity of the subducting Nazca plate could influence the dynamics of plate interfaces (Heuret and

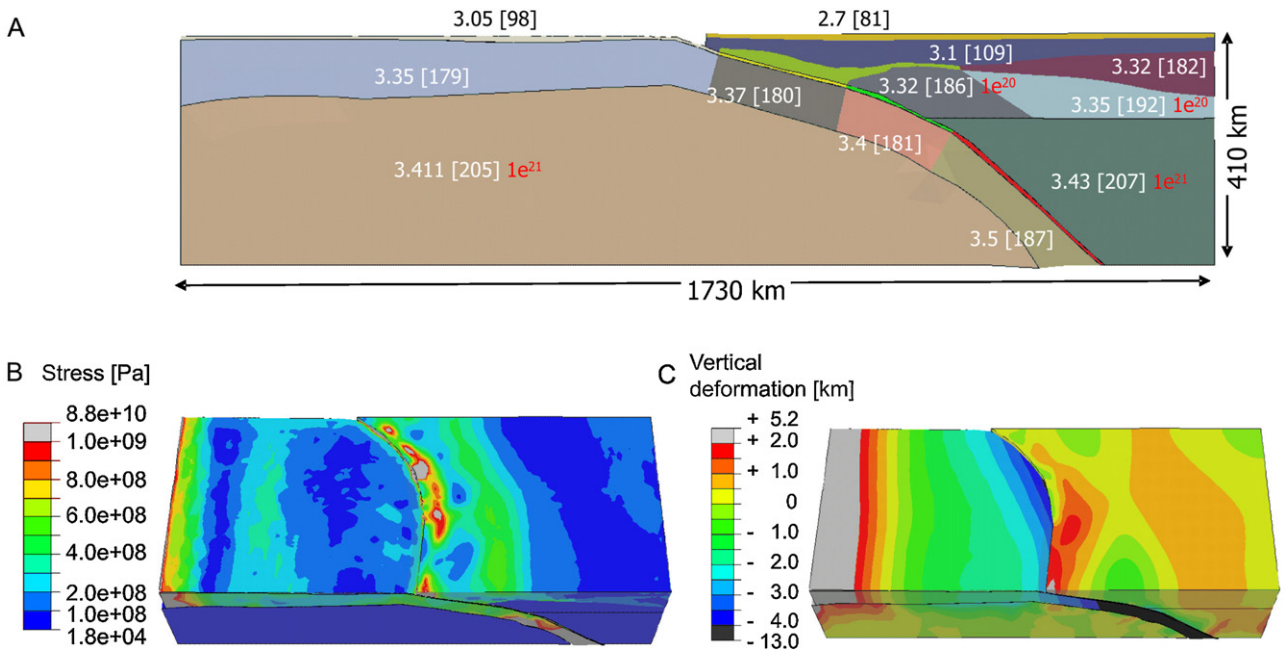

Fig. 9. Used parameters for the viscous-elastic model (A). Densities [$\times 10^3$ kg/m^3], Young's moduli [GPa] in brackets, viscosity in red. Oceanic crust: 3.2 [113] yellow, 3.3 [116] green, 3.55 [125] red, mantle wedge 3.23 [160] olive. Vertical deformations (B) and stress distribution (C).

Lallemand, 2005). In order to study the effects of these controlling parameters, rheologies (e.g. plasticity, viscoelasticity and visco-elasto-plasticity) and temperature on the dynamics of the thrust zone area, more generalized and realistic 3D models have been developed.

Fig. 9b shows the resulting vertical deformations. The calculated uplift is ~1.5 km and this corresponds to 7.5 mm/year. The expected surface uplift is smaller than 2 mm/year (Klotz et al., 2006; Jordan et al., 1997). Though our model neglects erosion, the estimated uplift from the numerical modelling is in the right order of magnitude. Fig. 9c shows the stress distributions. The stress (high and low) tends to follow the trend of the earthquake distributions in the region. The green belt indicates where the slab is at depth of 100 km.

The present study shows that well constrained geometries are crucial for dynamic modelling. The availability of satellite-derived gravity data has significantly improved the density models of the Andean region lacking terrestrial data. This in turn refined the geometries and densities of the geodynamic models. In particular, the long wavelength satellite-derived gravity anomaly is suitable to constrain the deep structures of the models. The resulting stress fields and new petrologic models can help to improve the density structure of the static models. Thus, a direct link between the static and dynamic models could be established.

5. Conclusions

Thorough understanding and interpretation of dynamic processes associated with hazardous regions is one of the major research interests in geosciences. Combined gravity models can provide valuable information for density modelling and geological interpretation where terrestrial gravity data of high resolution are available. In this study, it is shown that gravity prediction and downward continuation in some areas, e.g. the mountain ranges over Costa Rica and Central Andes, could lead to large errors and reduce the reliability of gravity data. Gravity prediction based on topography may not be appropriate for those regions. This calls the need to improve reduction techniques such as Bouguer calculation, topographic correction as well as downward continuation. The satellite only models have low spatial resolution compared to terrestrial data. However, the resolution is sufficient for interpretation of large-scale structures. Especially, in frontier regions such as parts of the Andes or Central America, where terrestrial gravity data coverage is limited, these models are valuable.

3D modelling of synthetic gradients and invariants of subduction zones, using the Andean as case study, proved the applicability of gradient measurements for detection of the edge of geological structures. Therefore, gradients from GOCE mission can resolve structural information and improve interpretation of asperities.

The long term and complex geodynamic processes of subduction could only be fully understood if model predictions are constrained with surface observables such as satellite gravity data. In the present study, a geodynamic model of the Andean margin has been developed with a realistic geometry based on density model constrained by gravity data and other relevant prior information. The stress distributions in the fore-arc, as determined from the dynamic modelling, mostly coincide with the locations of the earthquake of the region.

Finally, mapping and interpretation of hazardous regions require good gravity database (among others) to constrain lithospheric and dynamic processes. Satellite gravity data provide globally best information about frontier regions. Therefore, it is possible to interpret structures globally without limitations and combine regional interpretation of different regions into a one big picture.

Acknowledgements

This research is one of several projects of the SPP 1257 (Mass transport and mass distribution in the system of the Earth) supported by the German Research Council (DFG).

References

Alasonati-Tašárová, Z., 2007. Towards understanding the lithospheric structure of the southern Chilean subduction zone (36°S–42°S) and its role in the gravity field. Geophys. J. Int. 170, 995–1014.

Allmendinger, R.W., Jordan, T.E., Kay, S.M., Isacks, B.L., 1997. The evolution of the Altiplano-Puna Plateau of the Central Andes. Annu. Rev. Earth Planet. Sci. 25, 139–174.
ANCORP Working Group, 2003. Seismic imaging of a convergent continental margin and plateau in the central Andes (Andean continental research project 1996 (ANCORP 96)). J. Geophys. Res. 108, 2328.
Andersen, O.B., Knudsen, P., 1998. Global marine gravity field from the ERS-1 and Geosat geodetic mission altimetry. J. Geophys. Res. 103, 8129–8137.
Aochi, H., Madariaga, R., Fukuyama, E., 2003. Constraint of fault parameters inferred from nonplanar fault modeling. Geochem. Geophys. Geosyst. 4, 16, 1020.
Arroyo, I.G., Husen, S., Flueh, E.R., Gossler, J., Kissling, E., Alvarado, G.E., 2009. Three-dimensional P-wave velocity structure on the shallow part of the Central CostaRican Pacific margin from local earthquake tomography using on- and offshore networks. Geophys. J. Int. 179, 827–849.
Babeyko, A.Y., Sobolev, S.V., Vietor, T., Oncken, O., Trumbull, R.B., 2006. Numerical study of weakening processes in the central Andean back-arc. In: Oncken, O., Chong, G., Franz, G., Giese, P., Götze, H.-J., Ramos, V.A., Strecker, M., Wigger, P. (Eds.), The Andes – Active Subduction Orogeny. Frontiers in Earth Science Series, vol. 1. Springer-Verlag, Berlin/Heidelberg/New York, pp. 495–512.
Barckhausen, U., Roeser, H.A., von Huene, R., 1998. Magnetic signature of upper plate structures and subducting seamounts at the convergent margin of Costa Rica. J. Geophys. Res. 103, 7079–7093.
Barthelmes, 2009. Definition of functionals of the geopotential and their calculation from spherical harmonic models. GFZ Scientific Technical Report STR09/02. http://icgem.gfz-potsdam.de.
Bohm, M., Lüth, S., Echtler, H., Asch, G., Bataille, K., Bruhn, C., Rietbrock, A., Wigger, P., 2002. The southern Andes between 36°S and 40°S latitude: seismicity and average seismic velocities. Tectonophysics 356, 275–289.
Bolge, L.L., Carr, M.J., Milidakis, K.I., Lindsay, F.N., Feigenson, M.D., 2009. Correlating geochemistry, tectonics, and volcanic volume along the Central American volcanic front. Geochem. Geophys. Geosyst. 10, Q12S18.
Boutelier, D.A., Oncken, O., 2010. The role of the plate margin curvature in the plateau build-up: consequences for the Central Andes. J. Geophys. Res. 115, B04402, doi:10.1029/2009JB006296.
Brasse, H., Kapinos, G., Mütschard, L., Alvarado, G.E., Worzewski, T., Jegen, M., 2009. Deep electrical resistivity structure of northwestern Costa Rica. Geophys. Res. Lett. 36, L02310.
Buske, S., Lüth, S., Meyer, H., Patzig, R., Reichert, C., Shapiro, S., Wigger, P., Yoon, M., 2002. Broad depth range seismic imaging of the subducted Nazca slab, north Chile. Tectonophysics 350, 273–282.
Cloos, M., 1992. Thrust-type subduction-zone earthquakes and seamount asperities: a physical model for seismic rupture. Geology 20, 601–604.
DeMets, C., Gordon, R.G., Argus, D.F., Stein, S., 1994. Effect of recent revisions to the geomagnetic reversal timescale. Geophys. Res. Lett. 21, 2191–2194.
DeShon, H.R., Schwartz, S.Y., Bilek, S.L., Dorman, L.M., Gonzalez, V., Protti, J.M., Flueh, E.R., Dixon, T.H., 2003. Seismogenic zone structure of the southern Middle America Trench, Costa Rica. J. Geophys. Res. 108, 14, 2491.
Fedi, M., Ferranti, L., Florio, G., Giori, I., Italiano, F., 2005. Understanding the structural setting in the Southern Apennines (Italy): insight from Gravity Gradient Tensor. Tectonophysics 397, 21–36.
Förste, C., Flechtner, F., Schmidt, R., Stubenvoll, R., Rothacher, M., Kusche, J., Neumayer, K.-H., Biancale, R., Lemoine, J.-M., Barthelmes, F., Bruinsma, J., König, R., Meyer, U., 2008. EIGEN-GL05C – a new global combined high-resolution GRACE-based gravity field model of the GFZ-GRGS cooperation. General Assembly European Geosciences Union, Vienna, Austria. Geophys. Res. Abstr. 10, 2008, Abstract No. EGU2008-A-06944.
Fuller, C.W., Willett, S.D., Brandon, M.T., 2006. Formation of forearc basins and their influence on subduction zone earthquakes. Geology 34, 65–68.
Giese, P., Asch, G., Brasse, H., Götze, H.-J., Haberland, C., Wigger, P., 1999. Procesos geodinámicos en los andes centrales, representados mediante observaciones geofsícas. In: Bonorino, G.G., Omarini, R., Viramonte, J. (Eds.), Geología del Noroeste Argentino, Relatorio, Tomo I. Salta, pp. 15–17.
Götze, H.-J., Lahmeyer, B., 1988. Application of three-dimensional interactive modelling in gravity and magnetics. Geophysics 53, 1096–1108.
Götze, H.-J., Krause, S., 2002. The Central Andean gravity high, a relic of an old subduction complex? J. South Am. Earth Sci. 14, 799–811.
Götze, H.-J., Lahmeyer, B., Schmidt, S., Strunk, S., 1994. The lithospheric structure of the central Andes (20°S–26°S) as inferred from interpretation of regional gravity. In: Reutter, K., Scheuber, E., Wigger, P. (Eds.), Tectonics of the Southern Central Andes. Springer-Verlag, Berlin/Heidelberg/New York, pp. 7–21.
Gutscher, M.A., Spakman, W., Bijwaard, H., Engdahl, E.R., 2000. Geodynamics of flat subduction: seismicity and tomographic constraints from the Andean margin. Tectonics 19, 814–833.
Hackney, R.I., Featherstone, W.E., 2003. Geodetic versus geophysical perspectives of the "gravity anomaly". Geophys. J. Int. 154, 35–43.
Hackney, R., Echtler, H., Franz, G., Götze, H.-J., Lucassen, F., Marchenko, D., Melnick, D., Meyer, S.S., Tašárová, Z., Tassara, A., Wienecke, S., 2006. The segmented overriding plate and coupling at the south-central Chile margin (36°S–42°S). In: Oncken, O., Chong, G., Franz, G., Giese, P., Götze, H.-J., Ramos, V.A., Strecker, M., Wigger, P. (Eds.), The Andes – Active Subduction Orogeny. Frontiers in Earth Science Series, vol. 1. Springer-Verlag, Berlin/Heidelberg/New York, pp. 355–374.
Heuret, A., Lallemand, S., 2005. Plate motions, slab dynamics and back-arc deformation. Phys. Earth Planet. In. 149, 31–51.
Holstein, H., Sherratt, E.M., Reid, A.B., 2007. Gravimagnetic field tensor gradiometry formulas for uniform polyhedra. SEG Tech. Prog. Exp. Abstr. 26, 750–754.
Husen, S., 1999. Local earthquake tomography of a convergent margin, North Chile. Ph.D. thesis. Christian-Albrechts University, Kiel, Germany.
Husen, S., Quintero, R., Kissling, E., Hacker, B., 2003. Subduction-zone structure and magmatic processes beneath Costa Rica constrained by local earthquake tomography and petrological modelling. Geophys. J. Int. 155, 11–32.
Jordan, T.E., Reynolds III, J.H., Erikson, J.P., 1997. Variability in age of initial shortening and uplift in the Central Andes. In: Ruddiman, W.F. (Ed.), Tectonic Uplift and Climate Change. Plenum Press, New York, pp. 41–61.
Kirby, S., Engdahl E.R., Denlinger, R., 1996. Intermediate-depth intraslab earthquakes and arc volcanism as physical expressions of crustal and uppermost mantle metamorphism in subducting slabs. In: Bebout, G.E., Scholl, D.W., Kirby, S.H., Platt, J.P. (Eds). Subduction: Top to Bottom. American Geophysical Union, Geophysical Monograph 96, Washington, DC, pp. 195–214.
Kirchner, A., Götze, H.-J., Schmitz, M., 1996. 3d-density modelling with seismic constraints in the central Andes. Phys. Chem. Earth 21, 289–293.
Klotz, J., Khazaradze, G., Angermann, D., Reigber, G., Perdomo, R., Cifuentes, O., 2001. Earthquake cycle dominates contemporary crustal deformation in Central and Southern Andes. Earth and Plan. Sci. Lett. 193 (3–4), 437–446, doi:10.1016/S0012-821X(01)00532-5.
Klotz, J., Abolghasem, A., Khazaradze, G., Heinze, B., Vietor, T., Hackney, R., Bataille, K., Maturana, R., Viramonte, J., Perdomo, R., 2006. Long-Term signals in the present-day deformation field of the central andes and constraints on the viscosity of the earth's upper mantle. In: Oncken, O., Chong, G., Franz, G., Giese, P., Götze, H.-J., Ramos, V.A., Strecker, M., Wigger, P. (Eds.), The Andes – Active Subduction Orogeny. Frontiers in Earth Science Series, vol. 1. Springer-Verlag, Berlin/Heidelberg/New York, pp. 65–89.
Lessel, K., 1997. Die Krustenstruktur der zentralen Anden in Nordchile (21°S–24°S), abgeleitet aus 3D-Modellierungen refraktionsseismischer Daten. Ph.D. thesis. Freie Universität Berlin, Berlin. Berliner Geow. Abh. Reihe B: Geophys., 31, 185 pp.
Li, X., Götze, H.-J., 2001. Ellipsoid, geoid, gravity, geodesy, and geophysics. Geophysics 66, 1660–1668.
Lonsdale, P., 2005. Creation of the cocos and nazca plates by fission of the farallon plate. Tectonophysics 404, 237–264.
Lücke, O.H., Götze, H.-J., Alvarado, G.E., 2010. A constrained 3D density model of the upper crust from gravity data interpretation for Central Costa Rica. Int. J. Geophys., 9.
Lüth, S., Wigger, P., Araneda, M., Asch, G., Bataille, K., Bohm, M., Bruhn, C., Giese, P., Lüth, S., Quezada, J., Rietbrock, A., 2003. A crustal model along 39°S from a seismic refraction profile – ISSA 2000. Revista Geologica de Chile 30, 83–101.
Madariaga, R., Cochard, A., 1996. Dynamic friction and the origin of the complexity of earthquake sources. Proc. Natl. Acad. Sci. U.S.A. 93, 3819–3824.
Marsan, D., 2006. Can coseismic stress variability suppress seismicity shadows? Insights from a rate-and-state friction model. J. Geophys. Res. 111, B06305, doi:10.1029/2005JB004060.
Mayer-Guerr, T., 2007. ITG-Grace03s: the latest GRACE gravity field solution computed in Bonn. In: GSTM+SPP Conference, October 15–17, Potsdam.
Meschede, M., Barckhausen, U., Worm, H.U., 1998. Extinct spreading on the cocos ridge. Terra Nova 10, 211–216.
Norabuena, E.O., Dixon, T.H., Stein, S., Harrison, C.G.A., 1999. Decelerating nazca–south America and nazca–pacific plate motions. Geophys. Res. Lett. 26, 3405–3408.
Oncken, O., Chong, G., Franz, G., Giese, P., Götze, H.-J., Ramos, V.A., Strecker, M., Wigger, P., 2006. The Andes – Active Subduction Orogeny. Frontiers in Earth Science Series, vol. 1. Springer-Verlag, Berlin/Heidelberg/New York.
Pail, R., Goiginger, H., Schuh, W.-D., Höck, E., Brockmann, J.M., Fecher, T., Gruber, T., Mayer-Gürr, T., Kusche, J., Jäggi, A., Rieser, D., 2010. Combined satellite gravity field model *GOCO01S* derived from GOCE and GRACE. Geophys. Res. Lett. 37, L20314, doi:10.1029/2010GL044906.
Pavlis, N.K., Factor, J., Holmes, S., 2007. Terrain-related gravimetric quantities computed for the next EGM. Proceedings of the 1st International Symposium of the International Gravity Field Service (IGFS), Istanbul 2006, Istanbul, Turkey. Harita Dergisi, 318–323, special issue.
Pavlis, N.K., Holmes, S.A., Kenyon, S.C., Factor, J.K., 2008. An Earth Gravitational Model to Degree 2160: EGM2008. In: European Geosciences Union General Assembly, April 13–18, Vienna, Austria.
Pedersen, L.B., Rasmussen, T.M., 1990. The gradient tensor of potential field anomalies: Some implications on data collection and data processing of maps. Geophysics 55, 1558–1566.
Prezzi, C.B., Götze, H.-J., Schmidt, S., 2009. 3D density model of the Central Andes. Phys. Earth Planet. In. 177, 217–234.
Ramos, V., Aleman, A., 2000. Tectonic evolution of the Andes. In: Cordani, U., Milani, E., Thomaz Filho, A., Campos, D.A. (Eds.), Tectonic Evolution of South America. 31st International Geological Congress. Rio de Janeiro, pp. 635–685.
Ranero, C.R., von Huene, R., 2000. Subduction erosion along the middle America convergent margin. Nature 404, 748–752.
Ranero, C.R., Phipps Morgan, J., McIntosh, K., Reichert, C., 2003. Bending related faulting and mantle serpentinization at the Middle America trench. Nature 425, 367–373.
Reigber, C., Schmidt, R., Flechtner, F., König, R., Meyer, U., Neumayer, K.H., Schwintzer, P., Zhu, S.Y., 2005. An earth gravity field model complete to degree and order 150 from Grace: Eigen-grace02s. J. Geodyn. 39, 1–10.
Reichert, C., Schreckenberger, B., 2002. Cruise report SO-161 leg 2 & 3, SPOC (Subduction Processes Off Chile). Technical Report. BGR Hannover, 142 pp.

Reutter, K., Götze, H.-J., 1994. Comments on the geological and geophysical maps. In: Reutter, Scheuber, Wigger (Eds.), Tectonics of the Southern Central Andes. Springer, Heidelberg, pp. 329–333.
Sallarès, V., Dañobeitia, J.J., Flueh, E.R., 2001. Lithospheric structure of the Costa Rican Isthmus: effects of subduction zone magmatism on an oceanic plateau. J. Geophys. Res. 106, 621–643.
Sallarès, V., Charvis, P., Flueh, E.R., Bialas, J., 2003. Seismic structure of Cocos and Malpelo Volcanic Ridges and implications for hot spot-ridge interaction. J. Geophys. Res. 108, 2564.
Scheuber, E., Bogdanic, T., Jensen, A., Reutter, K., 1994. Tectonic development of the north Chilean Ande relation to plate convergence magmatism since the Jurassic. In: Reutter, K., Scheuber, E., Wigger, P. (Eds.), Tectonics of the Southern Central Andes. Springer, Berlin/Heidelberg/New York, pp. 7–22.
Schmidt, S., Götze, H.-J., 2006. Bouguer and isostatic maps of the Central Andes. In: Oncken, O., Chong, G., Franz, G., Giese, P., Götze, H.-J., Ramos, V.A., Strecker, M., Wigger, P. (Eds.), The Andes – Active Subduction Orogeny. Frontiers in Earth Science Series, vol. 1. Springer-Verlag, Berlin/Heidelberg/New York, pp. 559–565.
Schmidt, S., Götze, H.-J., Fichler, Ch., Alvers, M., 2010. IGMAS+ – a new 3D Gravity, FTG and Magnetic Modeling Software. Konferenzband GEO-INFORMATIK 2010 Die Welt im Netz, Herausgeber. In: Zipf, A., Behncke, K., Hillen, F. Schefermeyer, J. (Eds.), Akademische Verlagsgesellschaft AKA GmbH, pp. 57–63, ISBN:978-3-89838-335-6.
Schmitz, M., Lessel, K., Giese, P., Wigger, P., Araneda, M., Bribach, J., Graeber, F., Grunewald, S., Haberland, C., Lüth, S., Röwer, P., Ryberg, T., Schulze, A., 1999. The crustal structure beneath the central andean fore-arc and magmatic arc as derived from seismic studies – the PISCO 94 experiment in northern Chile (21°–23°S). J. South Am. Earth Sci. 12, 237–260.
Sick, C., 2006. Structural investigations of Chile: Kirchhoff Prestack Depth Migration versus Fresnel Volume Migration. Ph.D. thesis. Department of Earth Sciences, Free University Berlin, Berlin.
Sobiesiak, M., Meyer, U., Schmidt, S., Götze, H.-J., Krawczyk, C.M., 2007. Asperity generating upper crustal sources revealed by b-value and isostatic residual anomaly grids in the area of Antofagasta, Chile. J. Geophys. Res. 112, B12308.
Sobolev, S.V., Babeyko, A.Y., Koulakov, I., Oncken, O., 2006. Mechanism of the Andean Orogeny: insight from numerical modeling. In: Oncken, O., Chong, G., Franz, G., Giese, P., Götze, H.-J., Ramos, V.A., Strecker, M.R., Wigger, P. (Eds.), The Andes – Active Subduction Orogeny. Springer, pp. 513–535.
Somoza, R., 1998. Updated Nazca (Farallon)-South America relative motions during the last 40 My: implications for mountain building in the central Andean region. J. South Am. Earth Sci. 11 (3), 211–215.
Song, T.R.A., Simons, M., 2003. Large trench-parallel gravity variations predict seismogenic behavior in subduction zones. Science 301, 630–633.
Tassara, A., Götze, H.J., Schmidt, S., Hackney, R., 2006. Three-dimensional density model of the nazca plate and the andean continental margin. J. Geophys. Res. 111, B09404.
Tassara, A., 2010. Control of forearc density structure on megathrust shear strength along the Chilean subduction zone. Tectonophysics 495 (1–2), 34–47.
Wells, R.E., Blakely, R.J., Sugiyama, Y., Scholl, D.W., Dinterman, P.A., 2003. Basin-centred asperities in great subduction zone earthquakes: a link between slip, subsidence, and subduction erosion? J. Geophys. Res. 108, 30.